Sustainable Energy & Fuels

Application of highly stable biochar catalysts for efficient pyrolysis of plastics: a readily accessible potential solution to a global waste crisis

Journal:	*Sustainable Energy & Fuels*
Manuscript ID	SE-ART-04-2020-000652.R2
Article Type:	Paper
Date Submitted by the Author:	22-Jun-2020

Complete List of Authors:	Wang, Chenxi; Washington State University, Department of Biological Systems Engineering Lei, Hanwu; Washington State University, Dept. Biological Systems Engineering Qian, Moriko; Washington State University, Dept. of Biological Systems Engineering Huo, Erguang; Washington State University Zhao, Yunfeng; Washington State University Zhang, Qingfa; Washington State University Mateo, Wendy; Washington State University, Biological Systems Engineering Lin, Xiaona; Washington State University, Kong, Xiao; Washington State University Zou, Rongge; Washington State University Ruan, Roger; Center for Biorefining and Department of Bioproducts and Biosystems Engineering, University of Minnesota, 1390 Eckles Ave., Bioproducts and Biosystems Engineering

Application of highly stable biochar catalysts for efficient pyrolysis of plastics: a readily accessible potential solution to a global waste crisis

Chenxi Wang[a], Hanwu Lei[a,*], Moriko Qian[a], Erguang Huo[a], Yunfeng Zhao[a], Qingfa Zhang[a], Wendy Mateo[a], Xiaona Lin[a], Xiao Kong[a], Rongge Zou[a], Roger Ruan[b]

[a] Department of Biological Systems Engineering, Washington State University, Richland, WA 99354-1671, USA.
[b] Center for Biorefining and Department of Bioproducts and Biosystems Engineering, University of Minnesota, 1390 Eckles Ave., St. Paul, MN 55108, USA.
Correspondence to: hlei@wsu.edu

Abstract: The biochar catalysts derived from corn stover and Douglas fir were employed for the catalytic pyrolysis of model low-density polyethylene (LDPE) and real waste plastics. The corn stover derived biochar resulted in the liquid yield of about 40 wt.% without the wax formation. The liquid product comprised about 60% of C_8-C_{16} aliphatic, 20% of mono-aromatic, and 20% of C_{17}-C_{23} aliphatic hydrocarbons. The gas yield was about 60 wt.% with 60-80 vol.% of H_2. The corn stover derived biochar tended to generate more H_2 gas, and by contrast, CH_4 formation was favored when employing Douglas fir derived biochar catalyst. As for the property of reused biochars, the biochar catalyst derived from corn stover showed much better activity and longer lifetime than Douglas fir derived biochar, which might arise from the different contents of inherent minerals in biochar catalysts. After 20 times of experimental reuses and recycles, the corn stover derived biochar still possessed high activity in degrading LDPE without the wax formation. And after 10-cycle reuses of Douglas fir derived biochar, the catalyst was still active but its activity level has sharply declined with the production of amounts of wax. Additionally, real packaging plastic wastes respectively consisting of LDPE, high-density polyethylene (HDPE), polypropylene (PP), polystyrene (PS) and polyethylene terephthalate (PET) also could be effectively converted into valuable hydrocarbons and gases through using biochar catalyst, which implied that the biochar catalysts could be applied to the conversion of these common waste plastics. The current study demonstrated a new and efficient conversion of various waste plastics to jet fuels and H_2 by using a powerfully simple, and long-life biochar

23 catalyst.

1. Introduction

Various plastic wares are nowadays extensively used in packaging, agricultural production, and industrial manufacture.[1] In the past 50 years, 9.1 billion tons of plastics were manufactured in the world owing to the frequent replacement of plastic products, along with a yearly increasing rate of 8.7%.[2,3] The ideal strategy to combat the escalating waste plastics crisis is to establish a circular economy where plastic products could be used for as long as possible and then recycled at the end of their use.[4] Biodegradable plastics are considered to be a promising alternative to replace current plastics. However, biodegradable polymers hold shortcomings compared to conventional plastics, such as poor thermal tolerance.[5] As of now, it continues to be a great challenge to completely replace petrochemical-based plastics with biodegradable ones or for 100% recyclable.[6,7] And more than 90% of waste plastics end up in landfills, incineration and escaping into oceans.[8-10] Estimate predicts that the oceans will hold more waste plastics than fishes by 2050 if current production and waste plastics management trends continue.[11] Studies have demonstrated that the microplastics could spread into the human food chain or be directly absorbed by humans.[12,13] Hence, human beings should seriously tackle this crisis and give waste plastics second life before it gets uncontrollable.

Thermal pyrolysis is a temperature-dependent process, which has a limited application on waste plastics conversion. Catalytic pyrolysis is being developed for the decomposition of waste plastics where catalysts are employed to lower reaction temperature, reduce energy consumption and optimize conversion rates and

product quality.[14,15] Catalyst plays a key role in the catalytic process of waste plastics. Conventional solid acidic zeolites such as HZSM-5, HY and FCC E-cat have been mostly studied for the pyrolysis of waste plastics.[16,17-20] However, from the viewpoint of practical use, solid acidic zeolites are not economically competitive because of the relatively high cost and serious coke deposition issues. Therefore, what is of the most interest is to search cheaper and highly active catalysts for the conversion of waste plastics.[21,22]

Biochar is defined as a low-cost carbonaceous material, which is generally derived from biomass and can be used as catalysts, catalyst supports, and adsorbents.[19,23-25] Besides, sewage sludge, microalgae, coal, and manures are also feedstocks to obtain biochar.[26] Biochar can be produced through conventional thermochemical conversion of biomass such as pyrolysis, gasification and hydrothermal liquefaction, etc.[24] Additionally, in the past decades, microwave-assisted pyrolysis has been demonstrated as a potential alternative to conventional pyrolysis for the production of biochar. Microwave pyrolysis showcases several advantages over conventional pyrolysis such as easy operation on instant on/off control, high energy efficiency and fast heating rate, etc., the cause of which can be mainly attributed to their different heating mechanisms. During the microwave process, the biomass is pyrolyzed by convective and conductive heating, and the hot spots could be generated to enhance the energy transfer.[23,27] The moisture in biomass can work as the microwave absorber,[27,28] which conveys that the microwave pyrolysis can accept relatively high moisture feedstocks, and exempts

the need for pre-drying step that pyrolysis generally requires. By far, the pilot-scale microwave-assisted pyrolysis has been performed in several research centers such as in University of Minnesota and Norwegian University of Life Sciences.[29-31] The resulting biochar from microwave pyrolysis is suggested to be more reactive characterized by surface area, porous volume, and surface functional groups, etc. as compared to that from conventional pyrolysis. Whereas the yield of microwave biochar is usually lower than that of conventional ones.[27,32] Besides, non-uniform electromagnetic field in microwave reactor cavity may cause in-homogenous heating resulting in fluctuant natures over biochar.[33]

Activated biochar or activated carbon could be obtained from biochar by employing physical and chemical activation methods.[34,35] Zhang et al. reported that the waste plastics could be converted into valuable transportation fuel over activated carbon, and declared that the carbon catalysts activated by different methods had a remarkable impact on the compositions of products.[36] Very recently, Lin et al. performed the waste plastics co-pyrolysis using iron-loaded bifunctional activated carbon and stated that this bifunctional catalyst exhibited excellent performance on the production of mono-aromatics due to the newly created acid sites.[37] Wendy et al. found that the sulfonated carbon catalysts showed great potential in the co-pyrolysis of biomass and plastics for the production of jet-fuel range hydrocarbons.[38] By contrast with activated carbon, biochar is cheaper and can be more eco-friendly produced, however, it has not been tested for waste plastics conversions. Therefore, it is of dramatic interest to study the application of raw

biochar in solving worldwide waste plastics crisis.

The present work is to develop a new and novel route for utilization of waste plastics and demonstrate the feasibility of employing biomass-derived biochar catalysts in the catalytic pyrolysis of waste plastics from a variety of waste plastic containers and packaging materials.

2. Experimental section

2.1 Materials

The biochar catalyst used in this study was produced via microwave-assisted pyrolysis of biomass. The corn stover (crop biomass), as an agricultural waste, was collected from a local farm in Pasco city of Washington State. The Douglas fir sawdust (wood biomass) was purchased from Bear Mountain Forest Products incorporated, USA. Prior to use, the corn stover and Douglas fir were air-dried, ground to 2~4 mm granules and then used without further treatment. Low-density polyethylene (LDPE, C: 85.7 wt.% and H: 14.3 wt.%) was purchased from Sigma-Aldrich Corporation (St. Louis, MO, USA), milled into powder with a size of less than 1.5 mm and used without further treatment. The real waste plastics are disposable market shopping bags (LDPE, HDPE), packaging boxes (PP, PS), and purified water bottles (PET).

2.2 Biochar catalyst preparation and characterizations

A Sineo MAS-II microwave synthesis workstation (Shanghai, China) was used to implement biomass pyrolysis. In a typical run, 30 g corn stover or Douglas fir was loaded into a three-necked quartz flask and then inflated with 400 mL/min N_2 for 15

112 min to create an oxygen-free atmosphere. After that, N_2 was used as carrier gas at a
113 flow rate of 100 mL/min. The microwave-assisted pyrolysis process lasted for 40 min
114 with a power input of 700 W. At last, about 6~7.5 g biochar catalysts could be
115 collected and subsequently used in the pyrolysis of plastics without further
116 treatment.

117 The biomass-derived biochar catalysts were subjected to the characterizations
118 of elemental analysis, N_2 adsorption-desorption, NH_3 temperature-programmed
119 desorption (NH_3-TPD), minerals analysis, scanning electron microscope (SEM) &
120 energy-dispersive X-ray spectroscopy (SEM-EDS), Thermo-gravimetric analysis (TGA),
121 and Fourier-transform infrared spectroscopy (FT-IR), details of which were stated in
122 Supplementary Information.

123 **2.3 Catalytic pyrolysis and products analysis**

124 The catalytic performance testing of biochar was carried out in a fixed bed
125 quartz tube furnace reactor (Thermal Fisher Scientific), as the schematic diagram
126 shows in Fig. 1. Biochar catalysts and plastic feedstock were first introduced into the
127 quartz tube (inner diameter of 20 mm; length of 600 mm), then purged with N_2 at a
128 flow of 300 mL/min for 15 min to create an oxygen-free environment. The biochar
129 catalyst bed was first placed into the furnace which was heated to a pre-set
130 temperature, and then the plastic feedstock feeding bed was pushed into the
131 furnace to be heated for about 2 min to achieve the desired temperature. During the
132 pyrolysis, N_2 was set at a flow of 50 mL/min to carry the volatiles flowing through the
133 biochar catalyst bed and then condensation system. The total reaction time was

controlled at 15 min. The liquid product yield was calculated based on plastics feeding by the mass difference of the condensation system before and after the reaction. In this study, the coke deposition was neglected due to a slight change in the mass of biochar catalysts based on current experimental results. The yield of gas was calculated by using the mass balance of liquid and wax products. The weight change of biochar was obtained by the difference of catalyst before and after the reaction. A central composite design (CCD) was adopted to investigate the optimized experimental conditions. According to the results of CCD, the biochar to feed ratios and temperatures were respectively set to 1.59, 2, 3, 4.41 and 529, 550, 600, 650, 671 °C.

The chemical composition of liquid products was determined by using an Agilent 7890A/5975C GC-MS system equipped with a DB-5 capillary column. The GC was initially maintained at 40 °C for 5 min, and then was heated to 280 °C at a heating rate of 10 °C/min and maintained for 5 min. 1 µL of the ethyl acetate diluted sample was injected into the GC with helium gas at the flow rate of 0.6 mL/min. The ion source temperature was 230 °C for the mass selective detector. The NIST automatic mass spectral search library was applied to interpret the compounds detected in liquid samples. The area percentage of compounds based on the GC/MS results was used to predict the product selectivity.

The non-condensable was collected in a Tedlar gas bag and analyzed by using an INFICON 3000 Micro-GC (INFICON Inc., Santa Clara, CA, USA) system with two channels of thermal conductivity detectors (TCD). The column type of channel A is

Molecular Sieve with a temperature of 100 °C using Argon as the carrier gas. The column type of channel B is Plot U with a temperature of 85 °C using Helium as the carrier gas. Channel A and channel B were respectively used to identify H_2, CH_4, CO and CO_2, C_2, C_3, C_4. The gas compounds with more than 4 carbon atoms (>C_4) were either not detected or negligible in this study.

3. Results and discussion

3.1 Biochar characterizations

As Fig. 2A and Fig. 2B shows, different textural structures present in corn stover and Douglas fir derived biochars. The corn stover derived biochar possesses granular surface morphology with heaped pores. And the Douglas fir derived biochar contains irregular porous channels. The FT-IR results are conveyed in Fig. S1, regarding the fresh biochar catalysts, the bands shift at 1000-1050, 1450-1470, 1700, and 2930 cm^{-1} can be respectively assigned to the vibrations of -C-O, -C=C, -C=O and -C-H groups. There were no obvious adsorption peaks observed for Douglas fir derived biochars, which correlated with lower content of oxygen compared to the biochar derived from corn stover (see Table 1). Fig. S2 offers the TGA profiles, it can be found that the weight loss of corn stover derived biochar (10.82%) is about two times higher than of Douglas fir derived biochar (5.26%), which could also prove that the corn stover derived biochar contained more functional groups. The EDS results in Fig S3 reveal that the content of surface elements varied with spots location, which presents the heterogeneous distribution of minerals over the biochar matrix. Table 1 offers that the carbon content of corn stover derived biochar was 64.32 wt.%, which

is much lower than that from Douglas fir derived biochar (90.38 wt.%). Whereas the oxygen content is, on the contrary, 32.25 wt.% and 7.56 wt.% of which are respectively detected in corn stover and Douglas fir derived biochars. The oxygen content also explains the reason that there are no obvious FT-IR adsorption peaks detected in Douglas fir derived biochars. The BET surface area of Douglas fir derived biochar (152.06 m^2/g) is about three times higher than that of the biochar derived from corn stover (56.46 m^2/g), both of which are mostly comprising micropores (respectively 54.39 and 148.32 m^2/g). The surface area difference of two types of biochars is suggested to arise from their textural structures, which can be proved by the SEM images. That is, the irregular porous channels contained in Douglas fir derived biochar could increase its surface area. Whereas most of the channels formed in corn stover derived biochar are heaped pores that make a restricted contribution to its surface area. It also can be seen that both corn stover and Douglas fir derived biochar catalysts hold weak acidity. And the biochar derived from corn stover shows a much stronger acidity (0.0772 mmol/g NH_3 adsorption) than the Douglas fir derived biochar (0.0045 mmol/g NH_3 adsorption). In contrast with activated carbon, the biochar usually has a limited surface area, surface functional groups, and acidity.[36,37] Minerals analysis reveals that the corn stover derived biochar is rich in Ca, P, K, Mg, S, etc., and the contents of which are much higher than that from Douglas fir derived biochar. The inherent mineral constituents and its derivatives on biochar play important roles in the catalytic process.[39,40] The minerals content may also account for the different catalytic performance of biochars derived

from different feedstocks. Also during the catalysis, metals deposited on catalysts matter a lot in dehydrogenation reaction, especially for catalytic reforming in petroleum refinery, which is an important way to generate hydrogen.

3.2 Catalytic pyrolysis of waste plastics over biochars

Model LDPE pyrolysis over corn stover derived biochar. Table 2 summarizes the liquid and gas products yield as a function of catalytic temperatures and catalyst to LDPE ratios. It was found that the yield of the liquid product increased to 22-42 wt.% from less than 10 wt.% of the non-catalytic process (Run 38 and Run 39). The dramatic interest is that the wax yield decreased significantly in the presence of corn stover derived biochar, and the yield of the gas product only had a slight change, which showed that the corn stover derived biochar effectively catalyzed the degradation of LDPE into the liquid product without enhancing the gases generation. Additionally, it can be found that LDPE could be completely degraded into liquid as the temperature rises to 600 °C. However, for activated carbon, the similar results can be achieved only at a typical temperature of 500 °C, which can be attributed to the restricted catalytic activity caused by its limited surface functional groups, and acidity, etc. For example, Zhang et al.[36] reported that the yield of liquid product was up to 73% for LDPE pyrolysis over activated carbon at the temperature of 500 °C, which was higher than the yield of 67% (529 °C, Run 9 in Table 2) from the present study. Whereas in the present study, the mixed slurry of liquid and solid wax was observed at room temperature, indicating that the deficient degradation of LDPE compared to that over activated carbon. The authors also claimed that around 90

area% of the composition of the liquid product consisting of jet fuel range hydrocarbons, which was much higher than that (about 57 area%, Fig. 3) achieved over the biochar in the present study. However, the H_2 concentration in gas product from the biochar as catalyst was 78.35 vol.%, excelling that (about 60 vol.%) from the activated carbon as the catalyst.[36]

The lifetime of the catalyst has a significant influence on the catalytic performance and capital and operational expenditures. Therefore, the spent biochar collected after Run 2 was assessed for 20 cycles of reuse from Run 18 to Run 37. Compared to fresh biochar catalysts, as the results in Table 2 show, the liquid yield decreased to around 30 wt.% free of wax as before, which expressed that the biochar still kept a high activity in cracking LDPE into light fractions after 20 cycles of reuse. Spent biochar catalyst also gave rise to a higher yield (about 70 wt.%) of the gas product when compared to that (about 60 wt.%) from fresh biochar catalyst. What is more, one can be seen from Run 18 and Run 37 in Table 2, the 20^{th} cycle of biochar reuse had almost the same products yield as the 1^{st} cycle of reuse. Therefore, it can be envisaged that this biochar catalyst could maintain a long time activity of cracking LDPE despite coke deposition, which can be ascribed to the fact that the deposited coke is also carbonaceous residue being of a similar matrix with biochar catalyst. Recently, it was reported that the activated carbon reuse were limited to three cycles,[36] which might be because that the prior activation process may result in the damage to the structure of carbon catalyst. The long-life property of biochar was also an important finding of this work. Moreover, compared with the

biochar catalyst, conventional zeolites such as HZSM-5 shows better performance in the catalytic pyrolysis of waste plastics. However, coke deposition may sharply decrease the activity of zeolites. Therefore, coke deposited zeolites need calcined regeneration at a high temperature in the presence of air, which is an energy-intensive process. For instance, Awad et al.[41] studied the effects of USY zeolite regeneration on the polyethylene cracking, and the results revealed that the BET surface area decreased by about 45% after 14 cycles of regeneration at 500 °C, which indicated the partial collapse of crystalline structure and the deposition of coke species on the extra-framework leading to the blocking of pores. The authors also declared that USY was still active in cracking polyethylene after 14 cycles of regeneration but its activity has gradually decreased. By contrast, several advantages have been noticed for biochar catalysts over zeolites, for example, biochar is simpler and cheaper to be manufactured and its activity could last much longer after coke deposition.

Table S1 and Fig. 3 display the chemical compositions of liquid product in each run. Based on the results, these compounds are classified into five fractions including C_8-C_{16} aliphatic hydrocarbons, monocyclic aromatic hydrocarbons, dicyclic aromatic hydrocarbons, C_{17}-C_{23} aliphatic hydrocarbons and other compounds, of which C_8-C_{16} aliphatic, mono-/di-cyclic aromatic hydrocarbons, and C_{17}-C_{23} aliphatics can be regarded as aviation kerosene and diesel range fuels, respectively. It can be also seen that amounts of alkenes were observed in liquid product, while previous publications indicated that only alkanes were detected in the liquid product of waste

plastics pyrolysis over activated carbon,[36,42] which could arise from the domination of free radical reaction caused by the higher pyrolysis temperature and low acidity of raw biochar. In the absence of biochar, the only little amount of liquid product was observed and most of the product was in the state of solid wax with more than 24 carbon atoms at room temperature. However, when biochar was employed at a temperature of 600 °C and 3 of catalyst/LDPE ratio (Run 2, Run 3, Run 5, Run 10 and Run 13), as concluded from Table S1 and Fig. 3, about 60% of aliphatic hydrocarbons and 20% of monocyclic aromatics were identified, which can be used as jet fuel range hydrocarbons or blending composition of jet fuel. Around 20% of the liquid product C_{17}-C_{23} were aliphatic hydrocarbons that were in the range of diesel fuels. During 20 cycles of reuse, it is noteworthy that above five fractions almost kept at a constant yield, which could also further prove that the reused biochar maintained a long-time activity. At 600 °C and biochar to LDPE ratio of 3, the content of the C_8-C_{16} aliphatics in reuse experiments were almost the same as that from fresh biochar. The reused biochar tends to produce more mono-aromatics and C_{17}-C_{23} aliphatic hydrocarbons than the fresh one. The liquid product compositions change along with different biochar/LDPE ratios and temperatures were shown and discussed in Fig. S4.

As depicted in Table S2 and Fig. 4, the H_2 and CH_4 generation over fresh biochar were respectively at the range of 60-80 vol.% and 15-20 vol.%. And other compositions accounted for about 10 vol.%. At the temperature of 600 °C and 3 of biochar to LDPE ratio, more than 70 vol.% content of H_2 was observed, which was significantly increased from 40 vol.% of the absence of catalyst, exposing that

biochar catalyst could effectively promote the cleavage of C-H bond, which could also explain the reason for amounts of olefins generated in the liquid product. Meanwhile, CH_4 content has been reduced from about 45 vol.% to less than 20 vol.%. It was also seen that the gas hydrocarbons like C_2 and C_3 were attenuated as the biochar was employed in the pyrolysis. For example, the concentration of C_2, C_3, and C_4+ was 4.20, 1.35, and 2.43 vol.% in Run 39, which were respectively reduced to 2.05, 0.68, and 2.18 vol.%. This suggested that the biochar could enhance the formation of H_2, while the generation of CH_4 and C_nH_m was suppressed. Lately, Young-Kwon et al. have performed waste plastics gasification over Ni loaded biochar catalysts, and evidenced that Ni/biochar could enhance H_2 generation by approximately 2-fold in contrast with Ni-loaded activated carbon and conventional Al_2O_3.[43] As Fig. 4 illustrated, during 20 cycles of reuse, H_2 output was almost kept at a constant content of about 50 vol.%, which was lower than that produced over fresh biochar but still higher than the non-catalytic process. The CH_4 production was facilitated from less than 20 vol.% to about 40 vol.% but was still at a little lower concentration when compared to the non-catalytic process. And the reused biochar resulted in almost the similar content of C_2, C_3, and C_4+ in contrast with that from the free of catalyst. This suggested that the activity of spent biochar had deteriorated in terms of intensifying the H_2 production, which could be rooted in the fact that the deposited coke weakened the exposure of active sites on biochar. The compositions of gas product change along with different biochar/LDPE ratios and temperatures were shown and discussed in Fig. S5.

Model LDPE pyrolysis over Douglas fir derived biochar. For comparison, the biochar derived from Douglas fir was also employed for model LDPE pyrolysis. The distribution of liquid, wax, and gas products for LDPE pyrolysis over Douglas fir derived biochar is presented in Table 3. The liquid product yield was at a range of 10-30 wt.%, which is much higher than that from the non-catalytic process (Run 38 and Run 39 of Table 2). Compared to non-catalytic pyrolysis at a temperature of 600 °C and biochar to LDPE ratio of 3, the yield of wax has dramatically decreased by more than 20 wt.%, but the gas yield only increased by about 10 wt.%. Run 18 to Run 27 were also performed for 10 cycles of reuse of spent biochar collected from Run 2. Compared to fresh biochar catalyst, the yield of the liquid was decreased to 10-15 wt.%, and the wax yield was increased to around 20 wt.%, indicating that the activity of spent biochar has reduced to a lower level after reuses. The yield of the gas product stayed around 70 wt.% which is similar to that over fresh biochar.

From the results shown in Table 2, it could be concluded that the corn stover derived biochar exerted a better activity than the biochar derived from Douglas fir in terms of degrading LDPE, as the solid wax was not observed for LDPE pyrolysis over corn stover derived biochar. This may put down to the different assay of minerals or its derivatives between the biochars respectively derived from corn stover and Douglas fir. As the Table 1 revealed, the content of Ca (10175 ppm), P (8937 ppm), K (39387 ppm), and Mg (4831 ppm) on corn stover derived biochar greatly exceeded that of the biochar (Ca: 1041 ppm, P: 241 ppm, K: 829 ppm, and Mg: 141 ppm) derived from Douglas fir. Published studies have demonstrated that activated carbon

modified by these minerals could improve the catalytic properties of carbon catalysts. For instance, Yue et al. found that the carbon catalyst activated by CaO could significantly lower the reaction temperature during the synthesis of diaryl ether, and the purity of the desired product was also enhanced.[44] Therefore, it is envisaged that the different degradation property characterized by the yield of solid wax under the same conditions can be attributed to the big difference of Ca content, as this content on corn stover derived biochar is almost ten times higher than that of the biochar derived from Douglas fir. The H_3PO_4-activated carbon has been widely studied to degrade waste plastics, as the P-OH on carbon could serve as active sites to promote the conversion of long-chain hydrocarbons into aromatics.[36,45] The KOH activated carbon catalyst was mainly characterized by promoting the hydrogen transfer process during plastics pyrolysis, which increased the yield of aromatics at the cost of alkenes.[19] Recently, Huo et al. declared that the MgO modified activated carbon could boost the selectivity toward alkylated phenols during the catalytic pyrolysis of biomass, and the hydrogen production was promoted in the catalytic pyrolysis of LDPE over a combined catalyst of MgO and activated carbon,[42,46] which may account for the different hydrogen production resulted from two biochars, as the content of Mg on the biochar derived from corn stover is about thirty-four times higher than that of Douglas fir derived biochar.

Fig. 5 and Table S3 display the compositions of liquid products. The content of C_8-C_{16} aliphatic hydrocarbons accounted for about 50% when pyrolysis temperature kept at 600 °C. At the temperature of 600 °C, the content of both monocyclic

354 aromatic and C_{17}-C_{23} aliphatic hydrocarbons maintained at 20-30%. Around 10%
355 content of dicyclic aromatic hydrocarbons was detected in Run 1, Run 6, Run 8 and
356 Run 17 with reaction temperatures of more than 650 °C. During 10 cycles of reuse,
357 the content of C_8-C_{16} aliphatic, monocyclic aromatic and C_{17}-C_{23} aliphatic
358 hydrocarbons were almost the same as that of fresh biochar. The liquid product
359 compositions change along with different biochar/LDPE ratios and temperatures
360 were shown and discussed in Fig. S6.

361 Fig. 6 and Table S4 exhibits the chemical constitution of the gas product. During
362 pyrolysis conducted over fresh biochar, the H_2 content fluctuated from a low of
363 about 50 vol.% to a high of about 70 vol.%. And CH_4 concentration located within the
364 range of 25-40 vol.%. Trace amounts of CO_x appeared to be caused by the release of
365 inherent oxygen-containing groups or adsorbents existing on biochar, which could be
366 evidenced by the descending content of CO_x during the reuse cycles (see Fig. 6 and
367 Fig. 4). Combined with the Table S2, it can be concluded that the corn stover derived
368 biochar was inclined to generate more H_2, whereas the biochar derived from Douglas
369 fir tended to produce more CH_4. Compared to fresh biochar catalysts, it was obvious
370 that H_2 generation has been attenuated within 40-45 vol.% content during 10 cycles
371 of reuse, also carrying a descending trend with the increase of reuse times. However,
372 CH_4 formation has been observably facilitated to around 45 vol.% content, and also it
373 seems that CH_4 concentration remained at about the current level being
374 independent of reuse cycles. At the same time, the generation of C_2, C_3, and C_4
375 compounds was intensified with the consumption of H, which in turn accounted for

the decreasing concentration of H_2. The compositions of gas product change along with different biochar/LDPE ratios and temperatures were shown and discussed in Fig. S7.

Corn stover and Douglas fir derived biochar have been also respectively employed to further test their performance to pyrolyze real plastics that are composed of LDPE, HDPE, PP, PS, and PET including market shopping bags, packaging boxes, and purified water bottles. The products yield, compositions of liquid and gas fractions are listed and discussed in Table S5.

3.3 Characterizations on reused biochars

Fig. 2A' and 2B' indicate the SEM images of reused biochars. It can be seen that two types of biochars were still in good framework despite many cycles of reuses. Additionally, pores and channels were created in 20 cycles reused corn stover derived biochar, which might arise from the reaction between biochar and pyrolytic volatiles. It can be found that the Douglas fir derived biochar displayed lamellar structure after 10 cycles of reuses. The property of holding a stable framework devoted a lot to the service life of biochar catalysts. By contract with fresh biochar, as Fig. S1 revealed, strong adsorption peaks at 1000-1050 cm^{-1} were enhanced in reused biochars, which were attributed to the C-O stretching vibration. For reused Douglas fir derived biochar, the peaks at 1350, 1470, 1700, and 2930 cm^{-1} were obviously different from the fresh biochar, which respectively arose from -C-H (bending vibration), -C=C, -C=O and -C-H (stretching vibration) groups. The peak around 3420 cm^{-1} of reused biochar was caused by the -O-H stretching vibration.

Table S6 in Supplementary Information showed the mineral analysis results of reused biochars. The used biochar derived from corn stover possessed much higher content of minerals than the used biochar derived from Douglas fir, for example, Ca (8039 *vs* 1845 ppm), P (8170 *vs* 195 ppm), K (29488 *vs* 746 ppm), and Mg (4127 *vs* 114 ppm). The mineral loss appeared especially for the alkali metals such as Ca, K, and Na. As seen for corn stover derived biochar, the concentration of Ca, K, and Na respectively declined to 8039, 29488, and 395 ppm from that of 10175, 39387, and 677 ppm for fresh biochar. Whereas relatively lower loss of P was observed to decrease to 8170 from 8937 ppm, which indicated that the P functionalized groups stayed in a stable state over degrading the model LDPE.

3.4 Insight into the reaction mechanism

The free radical and carbonium ion reaction mechanisms are generally accepted to be the dominating mechanism respectively for the thermal and catalytic cracking of hydrocarbons.[19,47-49] Herein, LDPE is taken as an example to study the reaction mechanism in present work. The long-chain alkanes (LDPE) first undergoes thermal decomposition, during which the free radical reaction mechanism dominates. As conveyed in Fig. 7, the free radical reaction progresses in three successive stages: chain initiation, propagation, and termination. In the first stage, the thermal shock leads to the formation of many smaller free radicals like H•, CH_3•, and C_mH_n•. The formed radicals subsequently proceed in the propagation stage that consists of H-abstraction, β-scission, and isomerization reaction steps. The H-abstraction is also termed H-transfer, which could result in the formation of H_2, CH_4, etc., and new

420 radicals through reactions of existing radicals and hydrocarbons. The C-H bonds in
421 the β-position with respect to the free electron of C_mH_n• radicals could decompose
422 (self H-abstraction) with the yield of H• and olefins, which is an important route
423 resulting in the formation of conjugated olefins. The resulting olefins can further
424 generate aromatics through cyclization and aromatization reactions. In the
425 isomerization stage, the carbonium ions with more stable properties tend to be
426 generated through free electron transfer. The C-C bonds locating in the β-position
427 could decompose into olefins and new radicals. The inter-reactions occur in the
428 termination stage with the formation of H_2, CH_4, and short-chain alkenes and alkanes
429 through the bonding of existing radicals.

430 The Bronsted and Lewis acid sites of biochar dominate in the initial stage of the
431 carbonium ion reaction mechanism. The proton addition into C=C double linkages
432 yields corresponding carbonium ions. Generally, carbonium ions can also be
433 generated starting from alkanes by reacting with formed carbonium ions.
434 Meanwhile, isomerization reaction may easily occur accompanied by the
435 transformation of primary carbonium ions into more stable secondary carbonium
436 ions. Afterward, the long-chain carbonium ions will undergo β-scission with the
437 formation of olefins and new carbonium ions. The newly formed carbonium ions
438 may progress in the next reaction cycle, or be converted into olefins through proton
439 return to the catalyst for recovering the acid sites. Naphthenic hydrocarbons can be
440 produced from resulting olefins through isomerization and cyclization. Then the
441 naphthenic hydrocarbons can be converted into aromatics and amounts of H_2 under

the catalysis of inherent metals in biochar catalysts. The dehydrogenation property of specific metals plays a key role in the process of catalytic reforming, which is also a primary way to produce H_2 in petroleum refinery.

4. Conclusions

In this work, biochar catalysts derived from renewable biomass were employed to the catalytic conversion of waste plastics into liquid fuels and gases rich in H_2. The liquid product comprised about 60% of C_8-C_{16} aliphatic, 20% of mono-aromatic, and 20% of C_{17}-C_{23} aliphatic hydrocarbons, which are compatible with aviation kerosene and diesel range fuels, respectively. And up to 78 vol.% concentration of H_2 was observed in the gas product. The biochars could promote H_2 generation and the production of CH_4 was attenuated at the same time. By contrast, the results showed the corn stover derived biochar was inclined to generate more H_2, whereas the biochar derived from Douglas fir tended to produce more CH_4. The corn stover derived biochar could maintain a noteworthy and stable activity in degrading LDPE despite 20 cycles of reuse. What is more, real waste plastics including market shopping bags, packaging boxes, and purified water bottles could also be effectively converted into valuable products over biochar catalysts. The present work offers a novel route by using a powerfully simple and long-life biochar catalyst to convert a variety of waste plastic containers and packaging materials to high-value fuels and H_2.

Conflicts of interest

There are no conflicts of interest to declare.

Acknowledgements

This study was supported by the Agriculture and Food Research Initiative Competitive Grant No. 2016-67021-24533 and 2018-67009-27904 from the National Institute of Food and Agriculture, United States Department of Agriculture. Author contributions: C. W.: Conceptualization, methodology, formal analysis, investigation, writing the original manuscript. H. L.: Conceptualization, funding acquisition, supervision, writing-review & editing. Q. M., E. H, and Y. Z.: Methodology, writing-review & editing. Q. Z., W. M., X. L. and X. K.: Validation, review & editing. R. Z. and R. R.: Review & editing. We would like to thank Dr. Aftab Ahamed for the GC/MS analysis. And we are also thankful for Dr. Valerie Lynch-Holm and Dan Mullendore from Franceschi Microscopy & Imaging Center (FMIC) for the help with SEM-EDS training and analysis.

References

1 B. Bai, Y. Liu, Q. Wang, J. Zou, H. Zhang, H. Jin and X. Li, *Renewable Energy,* 2019, **135,** 32-40.

2 D. He, Y. Luo, S. Lu, M. Liu, Y. Song and L. Lei, *Trends Anal. Chem.,* 2018, **109,** 163-172.

3 R. Geyer, J. R. Jambeck and K. L. Law, *Sci. Adv.,* 2017, **3,** e1700782.

4 A European Strategy for Plastics in a Circular Economy. http://eur-lex.europa.eu/legal-content/EN/TXT/? qid=1516265440535&uri=COM:2018:28:FIN. (European Commission, 2018).

5 Editorial article, *Nat. Commun.,* 2018, **9:2157**, doi: 10.1038/s41467-018-04565-2.

6 A. C. Albertsson and M. Hakkarainen, *Science,* 2017, **358,** 872-873.

7 M. A. Hillmyer, *Science,* 2017, **358,** 868-870.

8 J. M. Garcia and M. L. Robertson, *Science,* 2017, **358,** 870-872.

9 W. Chen, K. Jin and N. L. Wang, *ACS Sustainable Chem. Eng.,* 2019, **7,** 3749-3758.

10 J. R. Jambeck, R. Geyer, C. Wilcox, T. R. Siegler, M. Perryman, A. Andrady, R. Narayan and K. L. Law, *Science,* 2015, **347,** 768-771.

11 D. E. MacArthur, *Science,* 2017, **358,** 843-843.

12 Y. Qi, X. Yang, A. M. Pelaez, E. H. Lwanga, N. Beriot, H. Gertsen, P. Garbeva and V. Geissen, *Sci. Total Environ.,* 2018, **645,** 1048-1056.

13 K. D. Cox, G. A. Covernton, H. L. Davies, J. F. Dower, F. Juanes and S. E. Dudas, *Environ. Sci. Technol.,* 2019, **53,** 7068-7074.

14 S. D. A. Sharuddin, F. Abnisa, W. M. A. W. Daud and M. K. Aroua, *Energy Convers. Manage.,* 2016, **115,** 308-326.

15 H. W. Lee and Y. K. Park, *Catalysts,* 2018, **8,** 501-515.

16 B. Kunwar, H. Cheng, S. R. Chandrashekaran and B. K. Sharma, *Renewable Sustainable Energy Rev.,* 2016, **54,** 421-428.

17 S. M. Al-Salem, A. Antelava, A. Constantinou, G. Manos and A. Dutta, *J. Environ. Manage.,* 2017, **197,** 177-198.

18 K. Ding, S. Liu, Y. Huang, S. Liu, N. Zhou, P. Peng, Y. Wang, P. Chen and Roger Ruan, *Energy Convers. Manage.,* 2019, **196,** 1316-1325.

19 K. Sun, Q. Huang, M. Ali, Y. Chi and J. Yan, *Energy Fuels,* 2018, **32,** 5471-5479.

20 X. Zhang, H. Lei, G. Yadavalli, L. Zhu, Y. Wei and Y. Liu, *Fuel,* 2015, **144,** 33-42.

21 J. M. Garcia, *Chem.,* 2016, **1,** 813-819.

22 A. Lopez, I. Marco, B. M. Caballero, M. F. Laresgoiti, A. Adrados and A. Aranzabal, *Appl. Catal. B.,* 2011, **104,** 211-219.

23 Y. Huang, P. Chiueh, C. Shih, S. Lo, L. Sun, Y. Zhong and C. Qiu, *Energy,* 2015, **84,** 75-82.

24 J. Cha, S. Park, S. Jung, C. Ryu, J. Jeon, M. Shin and Y. Park, *J. Ind. Eng. Chem.,* 2016, **40,** 1-15.

25 J. Wang and S. Wang, *J. Cleaner Prod.,* 2019, **227,** 1002-1022.

26 M.J. Ahmed and B.H. Hameed, *J. Cleaner Prod.,* 2020, **265,** 121762.

27 J. Li, J. Dai, G. Liu, H. Zhang, Z. Gao, J. Fu, Y. He and Y. Huang, *Biomass Bioenergy,* 2016, **94,** 228-244.

28 W. Ao, J. Fu, X. Mao, Q. Kang, C. Ran, Y. Liu, H. Zhang, Z. Gao, J. Li, G. Liu and J. Dai, *Renewable Sustainable Energy Rev.,* 2018, **92,** 958-979.

29 B. Zhang, S. Xiu and A. Shahbazi, *Nova Science Publishers Inc.,* 2012, doi: 10.13140/2.1.1953.7282.

30 C. Karunanithy and K. Muthukumarappan, *Biofuel's Engineering Process Technology,* doi: 10.5772/17621.

31 Q. H. Lin, H. Cheng and G. Y. Chen, *J. Anal. Appl. Pyrolysis,* 2011, **93,** 113-119.

32 C. Wu, V. L. Budarin, M. Wang, V. Sharifi, M. J. Gronnow, Y. Wu, J. Swithenbank, J. H. Clark and P. T. Williams, *Appl. Energy,* 2015, **157,** 533-539.

33 Y. Huang, P. Chiueh and S. Lo, *Sustainable Environ. Res.,* 2016, **26,** 103-109.

34 X. Cao, S. Sun and R. Sun, *RSC Adv.,* 2017, **7,** 48793-48805.

35 P. G. Garcia, *Renewable Sustainable Energy Rev.,* 2018, **82,** 1393-1414.

36 Y. Zhang, D. Duan, H. Lei, E. Villota and R. Ruan, *Appl. Energy,* 2019, **251,** 113337.

37 X. Lin, H. Lei, E. Huo, M. Qian, W. Mateo, Q. Zhang, Y. Zhao, C. Wang and E. Villota, *Energy Convers. Manage.,* 2020, **211,** 112757.

38 W. Mateo, H. Lei, E. Villota, M. Qian, Y. Zhao, E. Huo, Q. Zhang, X. Lin, C. Wang and Z. Huang, *Bioresour. Technol.,* 2019, **297,** 122411.

39 X. Xu, Y. Zhao, J. Sima, L. Zhao, O. Masek and X. Cao, *Bioresour. Technol.,* 2017, **241,** 887-899.

40 L. Zhang, Z. Bao, S. Xia, Q. Lu and K. Walters, *Catalysts,* 2018, **8,** 659-703.

41 C. Kassargy, S. Awad, G. Burnens, G. Upreti, K. Kahine and M. Tazerout, *Appl. Catal. B.,* 2019, **244,** 704-708.

42 E. Huo, H. Lei, C. Liu, Y. Zhang, L. Xin, Y. Zhao, M. Qian, Q. Zhang, X. Lin, C. Wang, W. Mateo, E. M. Villota and Roger Ruan, *Sci. Total Environ.,* 2020, **727,** 138411.

43 S. Park, J. Jae, A. Farooq, E. E. Kwon, E. D. Park, J. M. Ha, S. C. Jung and Y. K. Park, *Appl. Energy,* 2019, **255,** 113801.

44 Y. Han, G. Wang, W. Qiu, Y. Guo, Y. Sun, Y. Zhang, H. Zhou and T. Zhao, *Asian J. Org. Chem.,* 2018, **7,** 2511-2517.

45 K. Sun, Q. Huang, X. Meng, Y. Chi and J. Yan, *Energy Fuels,* 2018, **32,** 9772-9781.

46 E. Huo, D. Duan, H. Lei, C. Liu, Y. Zhang, J. Wu, Y. Zhao, Z. Huang, M. Qian, Q. Zhang, X. Lin, C. Wang, W. Mateo, E. M. Villota and R. Ruan, *Energy,* 2020, **199,** 117459.

543 47 P. A. Willems and G. F. Froment, *Ind. Eng. Chem. Res.,* 1988, **27,** 1959-1966.
544 48 Y. Xiao, J. M. Longo, G. B. Hieshima and R. J. Hill, *Ind. Eng. Chem. Res.,* 1997, **36,** 4033-4040.
545 49 A. G. Buekens and H. Huang, *Resour. Conserv. Recycl.,* 1998, **23,** 163-181.

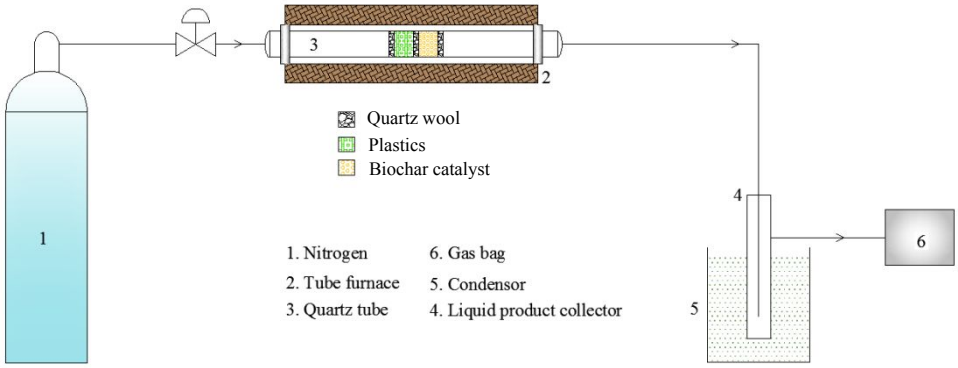

Fig. 1 The schematic diagram of the tube furnace pyrolysis system.

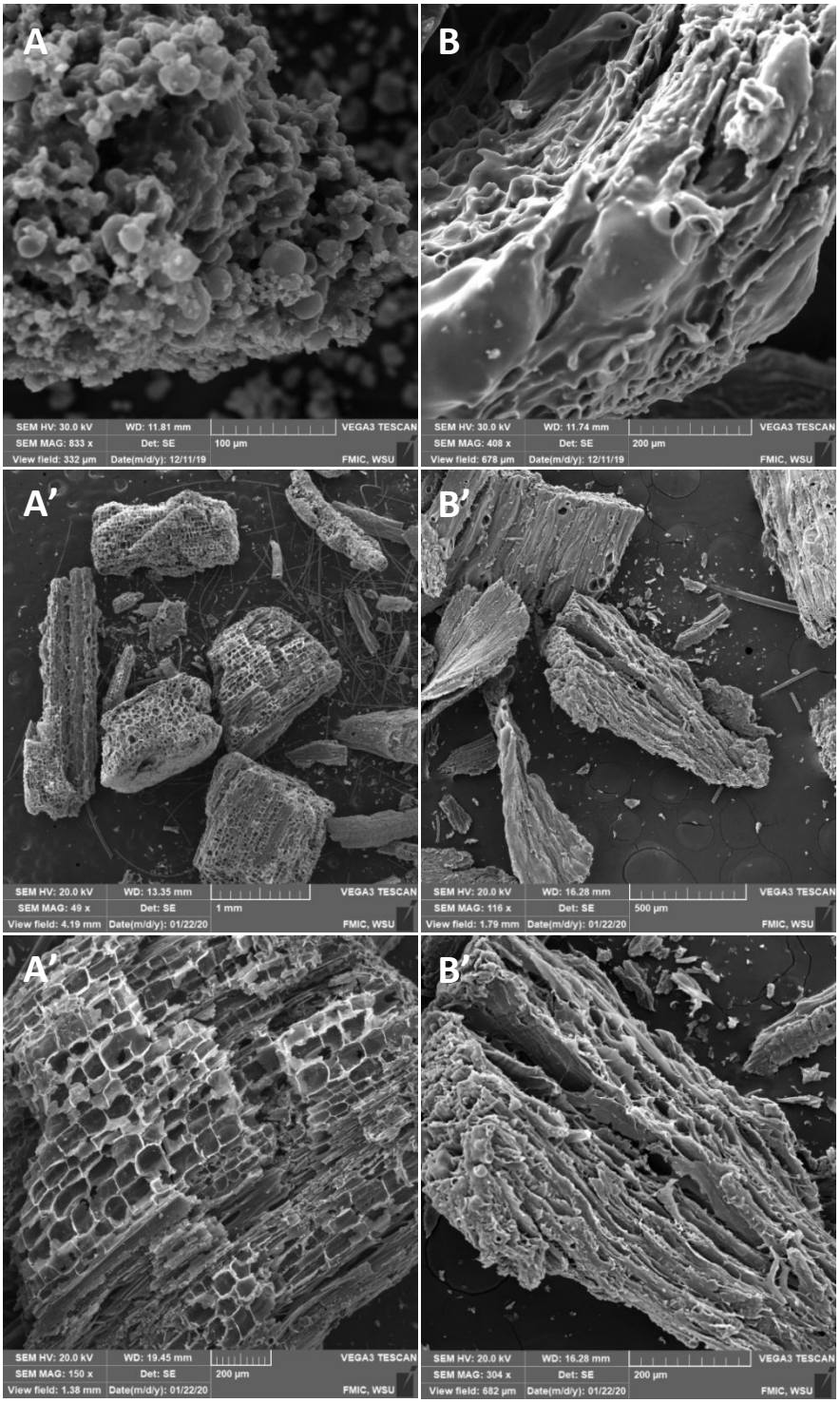

Fig. 2 SEM images of biochar: (A) fresh corn stover derived biochar; (B) fresh Douglas fir derived biochar; (A′) corn stover derived biochar after 20 cycles of reuse; (B′) Douglas fir derived biochar after 10 cycles of reuse.

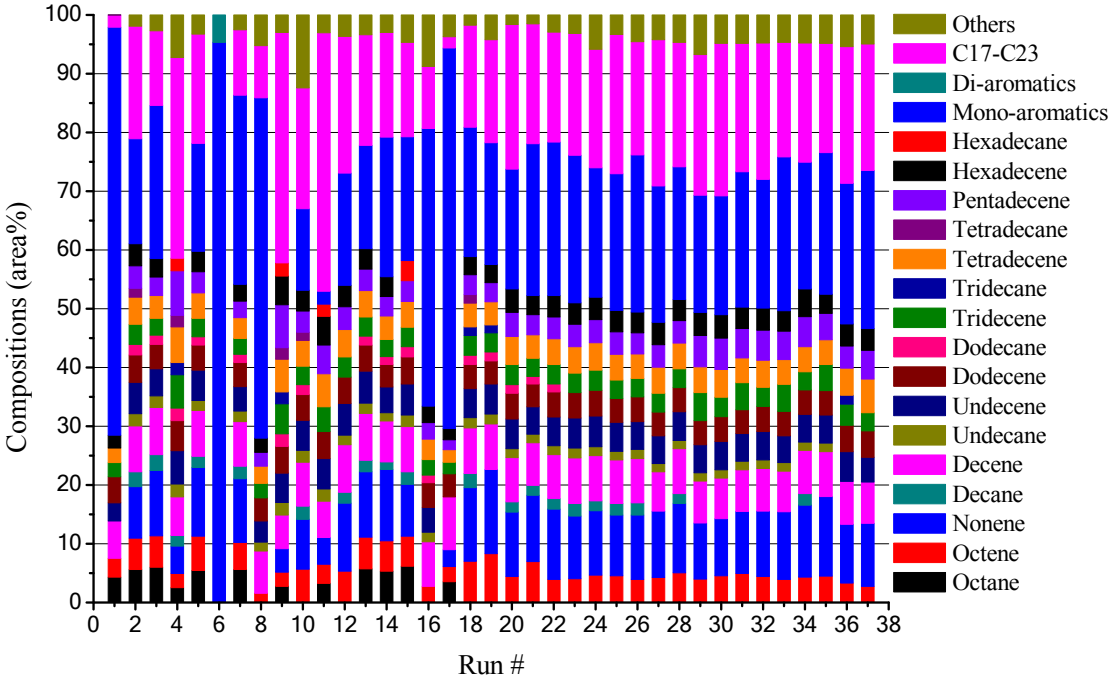

Fig. 3 Liquid product compositions of model LDPE pyrolysis over corn stover derived biochar.

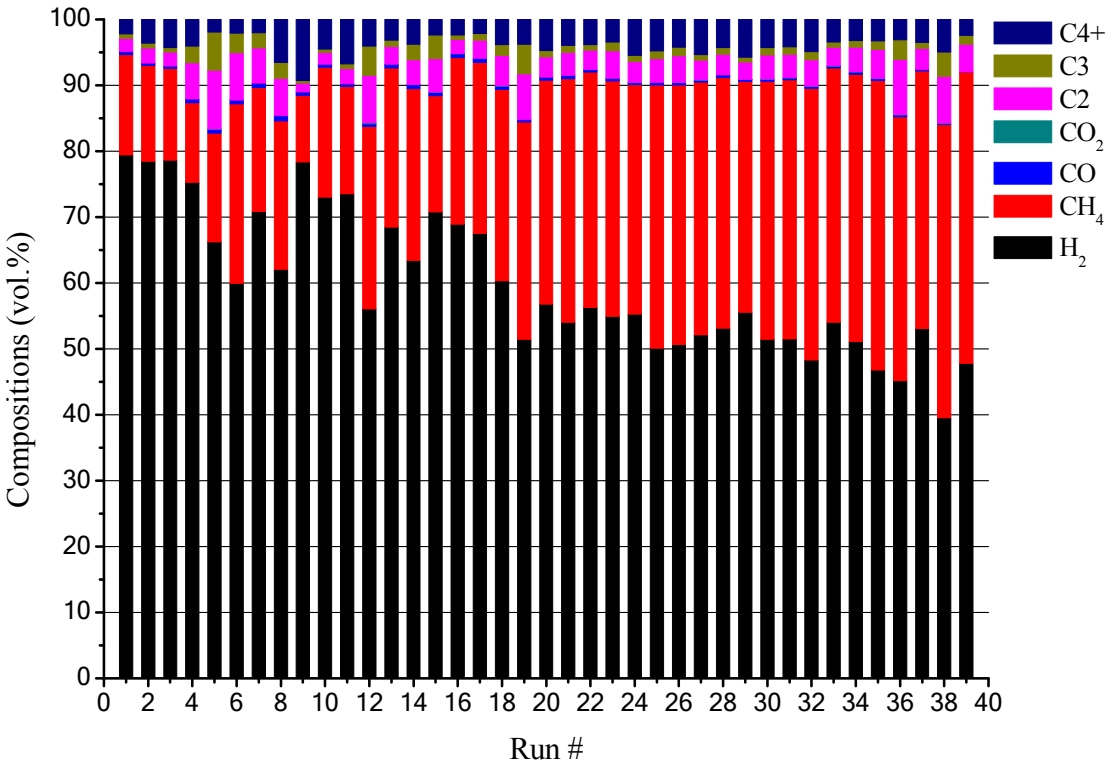

Fig. 4 Gas product compositions of model LDPE pyrolysis over corn stover derived biochar.

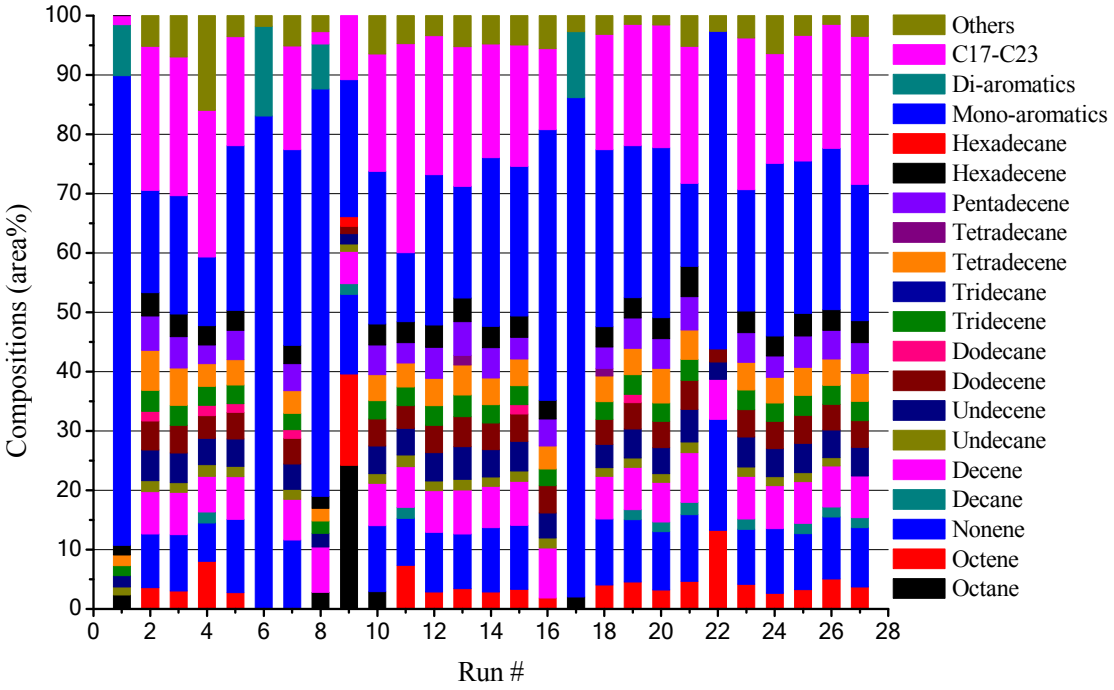

Fig. 5 Liquid product compositions of model LDPE pyrolysis over Douglas fir derived biochar.

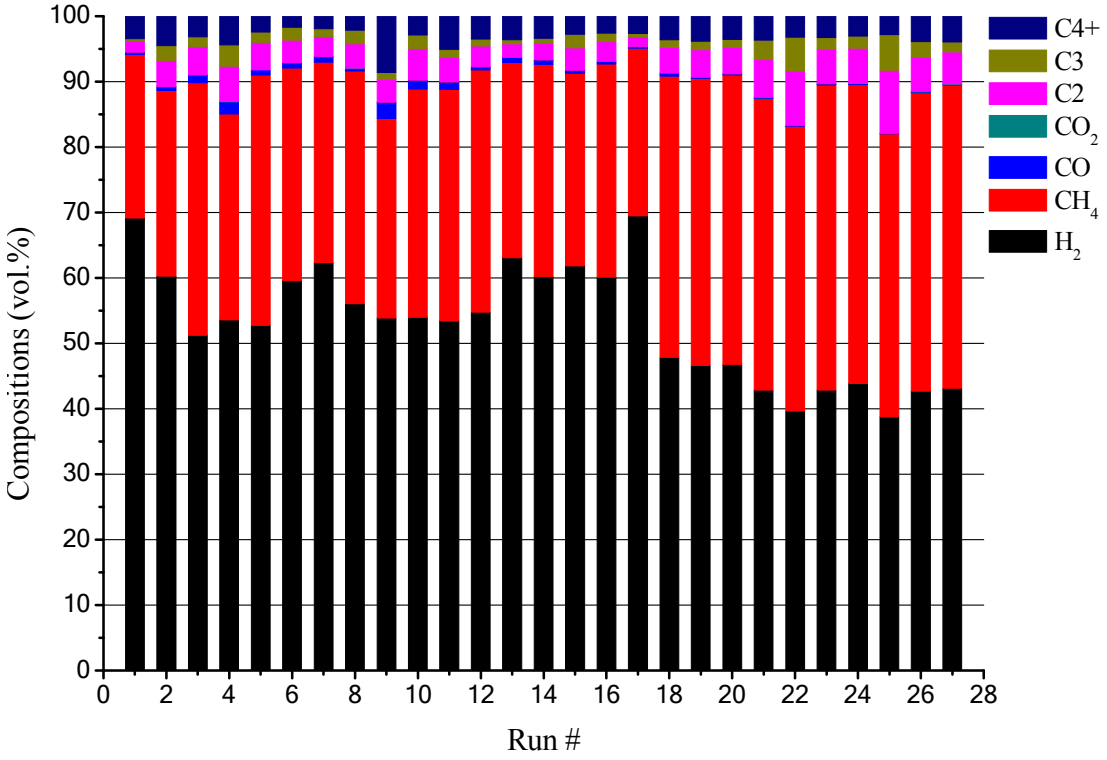

Fig. 6 Gas product compositions of model LDPE pyrolysis over Douglas fir derived biochar.

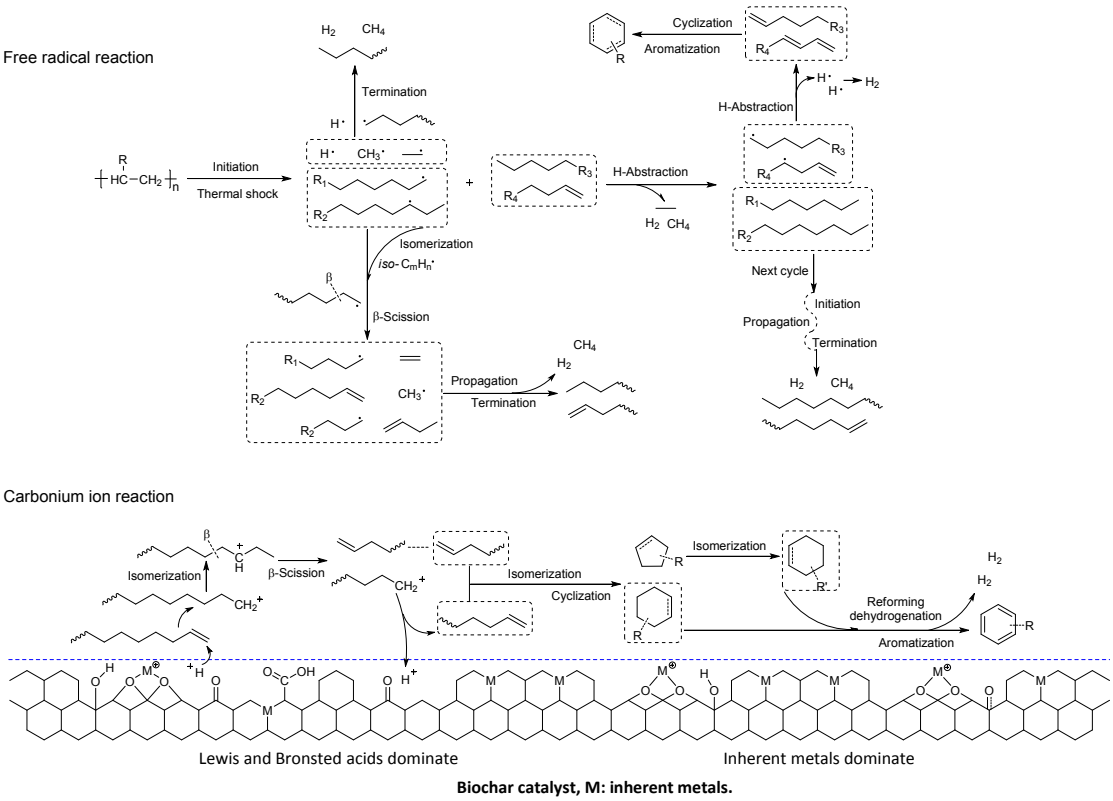

Fig. 7 The possible reaction mechanism for LDPE pyrolysis over biochar catalyst.

Table 1 Properties of corn stover and Douglas fir derived biochar.

Biochar derivation	Elemental analysis (wt.%)				Porous character (m^2/g)			NH_3-TPD	Complete mineral profile (ppm)										
	C	H	N	O*	S_{BET}	S_{micro}	S_{ext}	$NH_{3(ad)}$ (mmol/g)	Ca	P	K	Fe	Mg	Mn	S	Cu	Zn	Na	Al
Corn stover	64.32	1.24	2.19	32.25	56.46	54.39	2.08	0.0772	10175	8937	39387	159	4831	209	1532	9.30	43.0	677	117
Douglas fir	90.38	1.43	0.63	7.56	152.06	148.32	3.75	0.0045	1041	241	829	782	141	75.9	15.2	2.60	3.07	200	103

*By difference

Table 2 Products distribution of model LDPE pyrolysis over corn stover derived biochar.

Run[a]	Temperature/°C	Catalyst/feed mass ratio	Yield/wt.%			Weight change of biochar, Δ/g
			Liquid	Wax	Gas	
1	650.0	4.0	27.0	0	73.0	-0.19
2	600.0	3.0	42.0	0	58.0	-0.08
3	600.0	3.0	40.0	0	60.0	-0.15
4	550.0	4.0	43.0[s]	-	57.0	-0.05
5	600.0	3.0	38.0	0	62.0	-0.09
6	671.0	3.0	22.0	0	78.0	-0.23
7	600.0	4.4	24.0	0	76.0	-0.13
8	650.0	2.0	22.0	0	78.0	-0.05
9	529.0	3.0	67.0[s]	-	33.0	-0.2
10	600.0	3.0	41.0	0	59.0	-0.02
11	550.0	2.0	62.0[s]	-	38.0	-0.04
12	600.0	1.6	42.0[s]	-	58.0	-0.09
13	600.0	3.0	42.0	0	58.0	-0.12
14	600.0	2.5	35.0	0	65.0	-0.04
15	600.0	4.0	40.0	0	60.0	-0.1
16	625.0	3.0	23.0	0	77.0	-0.06
17	650.0	3.0	30.0	0	70.0	-0.04
18	600.0	3.0	31.0	0	69.0	0.02
19	600.0	3.0	35.0	0	65.0	0.03
20	600.0	3.0	25.0	0	75.0	0.05
21	600.0	3.0	30.0	0	70.0	0.03
22	600.0	3.0	26.0	0	74.0	-0.02
23	600.0	3.0	27.0	0	73.0	0
24	600.0	3.0	26.0	0	74.0	0
25	600.0	3.0	33.0	0	67.0	0.01
26	600.0	3.0	30.0	0	70.0	-0.02
27	600.0	3.0	26.0	0	74.0	-0.03
28	600.0	3.0	38.0	0	62.0	0.01
29	600.0	3.0	29.0	0	71.0	-0.03
30	600.0	3.0	30.0	0	70.0	-0.03
31	600.0	3.0	29.0	0	71.0	-0.01
32	600.0	3.0	31.0	0	69.0	0.01
33	600.0	3.0	26.0	0	74.0	-0.01
34	600.0	3.0	28.0	0	72.0	-0.01
35	600.0	3.0	31.0	0	69.0	0
36	600.0	3.0	28.0	0	72.0	-0.04
37	600.0	3.0	27.0	0	73.0	0.01
38	600.0	-	7.0	34.0	59.0	-
39	650.0	-	9.0	10.0	81.0	-

[a] Run 1 to Run 13 was conducted based on CCD; Run 14 to Run 17 was added as controls; Run 18 to Run 37 was performed to reuse the spent biochar catalyst from Run 2 for 20 cycles; Run 38 and Run 39 were controls in the absence of biochar.

[s] A mixture of liquid oil and solid wax at room temperature.

Table 3 Products distribution of model LDPE pyrolysis over Douglas fir derived biochar.

Run[a]	Temperature/°C	Catalyst/feed mass ratio	Yield/wt.%			Weight change of biochar, Δ/g
			Liquid	Wax	Gas	
1	650.0	4.0	17.0	0	83.0	-0.08
2	600.0	3.0	30.0	6.0	64.0	-0.04
3	600.0	3.0	29.0	5.0	66.0	-0.05
4	550.0	4.0	16.0	42.0	42.0	-0.08
5	600.0	3.0	23.0	6.0	71.0	-0.08
6	671.0	3.0	14.0	0	86.0	-0.06
7	600.0	4.4	32.0	0	68.0	-0.11
8	650.0	2.0	17.0	0	83.0	-0.04
9	529.0	3.0	10.0	61.0	29.0	-0.06
10	600.0	3.0	23.0	4.0	73.0	-0.07
11	550.0	2.0	10.0	45.0	45.0	-0.04
12	600.0	1.6	25.0	4.0	71.0	-0.05
13	600.0	3.0	29.0	5.0	66.0	-0.09
14	600.0	2.5	23.0	3.0	74.0	-0.08
15	600.0	4.0	26.0	3.0	71.0	-0.12
16	625.0	3.0	20.0	6.0	74.0	-0.07
17	650.0	3.0	16.0	0	84.0	-0.11
18	600.0	3.0	25.0	7.0	68.0	0
19	600.0	3.0	14.0	17.0	69.0	-0.01
20	600.0	3.0	13.0	14.0	73.0	-0.02
21	600.0	3.0	14.0	18.0	68.0	-0.01
22	600.0	3.0	7.0	25.0	68.0	-0.02
23	600.0	3.0	10.0	23.0	67.0	-0.03
24	600.0	3.0	15.0	11.0	74.0	-0.01
25	600.0	3.0	12.0	18.0	70.0	-0.02
26	600.0	3.0	13.0	17.0	70.0	-0.01
27	600.0	3.0	12.0	19.0	69.0	0.01

[a] Run 1 to Run 13 was conducted based on CCD; Run 14 to Run 17 were added as controls; Run 18 to Run 27 was performed to reuse the spent biochar catalyst from Run 2 for 10 cycles.

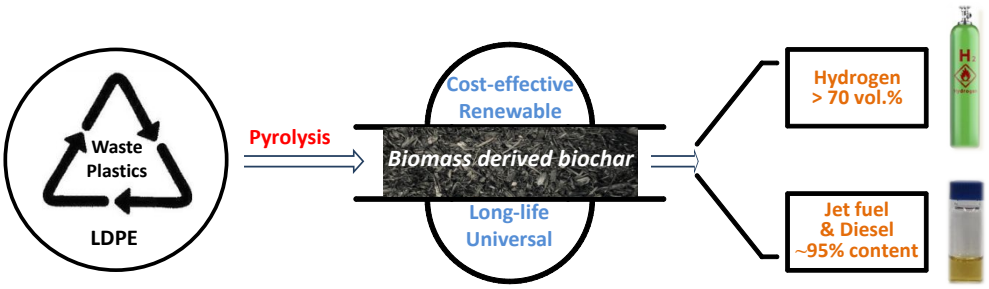
Waste
Plastics
LDPE
Pyrolysis
Cost-effective
Renewable
Biomass derived biochar
Long-life
Universal
Hydrogen
> 70 vol.%
Jet fuel
& Diesel
~95% content